Simulation of flow with spray closely to the air-blast injector: stochastic immersed body approach combined with LES

M. Gorokhovski*, T. Deng, C. Le Ribault*& R.Zamansky*****

*LMFA, Ecole Centrale de Lyon, Ecully, France
**Beihang University of Aeronautics (BUAA), Beijing, China
***Stanford University, CTR, USA

Abstract

In this paper, the new extension to the stochastic simulation of primary air-blast atomization is introduced, and it is assessed by comparison with measurements. The idea of this extension is as follows. In LES of the gas flow, the primary atomization zone (liquid core, network of filaments and detached primary blobs) is viewed as immersed porous solid body with the stochastic structure. Namely, such a composite body is flowing with the inlet parameters for the liquid jet, and it is changing randomly its configuration. The statistics of configuration of this immersed body are used as boundary conditions in LES of the gas flow, thereby it is assumed that the jet fragmentation process is faster than the typical time resolved scale in the gas flow. The statistical structure of the immersed body is defined by specifically introduced stochastic particles, moving in the space, and identifying the random position, outwards normal and curvature of the interface between the liquid and the gas. This numerical approach is assessed by comparison with experimental study of air-blast atomization, which was performed in LEGI (Grenoble, France). Two observations are worth noting. The first one is that the recirculation zone, in the front of the liquid core, and flapping of the liquid core may provoke the bursting production of small droplets. The second one is that resulting to the more intensive atomization process, the transversal gradients of velocity are decreasing with increasing the gas-to-liquid momentum ratio.

Introduction and Approach

In air-blast atomization, the liquid is injected at low pressure into a high-speed co-flow of the gas. Due to momentum exchange with the gas, the continuous liquid bulk forms a complex network of threads and ligaments; each has a large number of degrees of freedom, involving a broad range of length-and-time scales into the spray production. The different approaches were proposed to simulate such a process of atomization. The simplest one comprises the conventional Lagrangian models, which are in widespread use in industrial numerical codes. In these models, along with integration of governing equations for the gaseous phases, the round proliferating blobs (initially, of the nozzle exit diameter) are injected into computational domain, and are tracked with exchange of mass, momentum, and energy between the spray and the gas. The gas flow is computed either by RANS or by LES approaches. The presumed mechanisms of breakup of each tracking sphere include surface instabilities (Beale & Reitz, 1999), drop shedding (Yi & Reitz, 2004), spontaneous breakup (Tanner, 2004), turbulence (Huh & Gosman, 1991). Since the sizes of droplets may be predicted only with a certain probability, Gorokhovski (2001), Gorokhovski & Saveliev (2003), Apte et al. (2003), Jones & Lettieri (2010), Liu et al. (2006) proposed to simulate the droplet proliferation stochastically in the frame work of the same population balance equation. This population balance equation is based on assumption of fragmentation under scaling symmetry. Although the conventional models are simple in implementation for practical conditions, and they have non-diffusive character, the liquid flow in these models is mimicked by motion of round spheres, thereby its real complex dynamics and interactions with the gas is oversimplified. In Vallet et al. (2001), and later on in Jay et al., 2006, the primary atomization is described in lines of a single "fluid" RANS turbulent mixing of a high-density jet with an ambient gas. In this approach, in order to estimate the local mean radius of droplet, the transport equation is presumed for the mean interface density. This scalar is governed by mean convection, gradient-type diffusion, production (stretching) and destruction (coalescence). Another approach is based on the direct primary atomization modeling, and is focused on evolution of the gas/liquid interface (see, for example, review Gorokhovski & Hermann, 2008). This approach is promising though requiring in turn the significant CPU-resources. However, when the Weber number is high, this approach raises the following question (Hermann & Gorokhovski, 2008): what are the filtered equations of two-phase immiscible flow with the interface, and how to simulate this flow and the interface on subgrid scales. With respect to the mass and energy conservation, the unresolved scales become crucial for breakup modeling.

* Corresponding author: mikhael.gorokhovski@ec-lyon.fr

In this paper, we propose another, which is different from those referenced above. We simply replace the zone of primary atomization by a flowing immersed body, with the structure simulated stochastically by the fragmentation process evolving in the down-stream direction. The parameters of fragmentation are calculated dynamically with the flow evolution by presumed mechanism of atomization. The flow is supposed to be composite. It contains the connected (continuous) phase, and the disconnected (dispersed) phase. The connected phase is assumed to be governed by the following equations:

$$\frac{\partial \langle u_i \rangle}{\partial t} = \begin{cases} -\dfrac{\partial \langle u_i u_j \rangle}{\partial x_j} + \dfrac{1}{\rho_g}\dfrac{\partial \langle \sigma_{ij} \rangle}{\partial x_j}, \ if \ P_l = 0 \\ P_l \ \dot{u}_S n_i, \ if \ P_l \neq 0 \end{cases} \tag{1}$$

$$\frac{\partial \langle u_j \rangle}{\partial x_j} = 0 \tag{2}$$

where brackets $<...>$ denote filtering in terms of LES approach, thereby $\langle u_i \rangle$ denotes the filtered velocity filtered velocity component. The upper line in the right-hand side of (1) represents the constant property Navier-Stokes equation, in which σ_{ij} is the stress tensor in the gas flow. The bottom line in the right-hand side of (1) contains three variables: $P_l(\vec{x},t)$, $\dot{u}_S(\vec{x},t)$, $n_i(\vec{x},t)$. Here $P_l(\vec{x},t)$ is the probability to find the liquid flow at the given point in the primary atomization zone, $\dot{u}_S(\vec{x},t)$ is the local acceleration in this zone (it is assumed to be controlled by the local acceleration of the liquid/gas interface), and $n_i(\vec{x},t)$ is the component of unit orientation vector (will be also addressed to the local outwards normal of the liquid/gas interface). These three variables need to be modeled. The probability $P_l(\vec{x},t)$ is simulated by specifically introduced stochastic particles moving with the flow and simulating the liquid core depletion (Gorokhovski et al. 2009); each trajectory represents one realization of the liquid core configuration. To each such a particle, the interface normal $n_i(\vec{x},t)$ is prescribed, which is simulated in the framework of the stochastic relaxation towards isotropy in the down-stream direction: $n_i(\vec{x},t)$ evolves stochastically by Brownian motion on the unit sphere (Zamansky et al. 2010). The expression for $\dot{u}_S(\vec{x},t)$ is based on the increment of the interface velocity: $\dot{u}_S \, n_i = \dfrac{u_S^{n+1} n_i - \langle u_i \rangle^n}{\Delta t}$, where $u_S^{n+1} n_i$ denotes the interface velocity. Then in the sub-region with $0 < P_l < 1$, the above equation (1) is reduced to $\langle u_i \rangle^{n+1} = (1 - P_l)\langle u_i \rangle^n + P_l \, u_S^{n+1} n_i$; particularly, if $P_l = 1$ then $\langle u_i \rangle^{n+1} = u_S^{n+1} n_i$. In this study, the interface velocity is taken to be constant, and to be equal to the convection velocity: $u_S = \dfrac{\left(\sqrt{\rho_g}\, u_{g,0} + \sqrt{\rho_l}\, u_{l,0}\right)}{\left(\sqrt{\rho_g} + \sqrt{\rho_l}\right)}$ (Villermaux E., 1998), where $u_{g,0}$ is the inlet gas velocity, $u_{l,0}$ is the inlet liquid velocity. In terms of the immersed body force method (Grigoriadis et al., 2003), equation (1) can be written in discrete form:

$$\frac{\langle u_i \rangle^{n+1} - \langle u_i \rangle^n}{\Delta t} = \langle RHS_i \rangle + \langle F_i \rangle \tag{3}$$

where

$$\langle RHS_i \rangle = -\frac{\partial \langle u_i u_j \rangle}{\partial x_j} + \frac{1}{\rho_g}\frac{\partial \langle \sigma_{ij} \rangle}{\partial x_j} \quad \text{and} \quad \langle F_i \rangle = \begin{cases} 0, \ if \ P_l = 0 \\ -\langle RHS_i \rangle + P_l \ \dot{u}_S \ n_i, \ if \ P_l \neq 0 \end{cases}. \tag{4}$$

The difference with (Grigoriadis et al., 2003) is that the immersed body has spatially random structure; $P_l(\vec{x},t)$ is simulated dynamically with the flow evolution; thereby the velocity in the immersed body is not constant. The dispersed phase in the composite flow is conditioned by $0 < P_l(\vec{x},t) < 1$. It is presented by the motions of liquid drops; these motions are averaged over the inter-droplet collisions. The drops are tracked by:

$$\frac{d\,\overline{\mathrm{v}}_{\mathrm{p}}}{d\,t} = \begin{cases} \dfrac{\langle u_i \rangle - \overline{\mathrm{v}}_{\mathrm{p}}}{\tau_{St}} - \nabla \dfrac{T_p}{m_p}, \ if \ \ P_l \neq 0 \\ \dfrac{\langle u_i \rangle - \mathrm{v}_{\mathrm{p}}}{\tau_{St}}, \ if \ \ P_l = 0 \end{cases} \tag{5}$$

where $\overline{\mathrm{v}}_{\mathrm{p}}$ is the drop velocity averaged over collisions, T_p is the drop statistical temperature, and τ_{St} is the Stokes time. The model for statistical temperature T_p is also given hereafter. Assuming that blobs are stripped in the zone $0 < P_l(\vec{x},t) < 1$, their initial size can be sampled from simulated spatial distribution $n_i(\vec{x},t)$, namely by $\nabla \cdot \mathbf{n}$. However in this manuscript, we presumed the exponential distribution of size of formed blobs; the sampled drops are subject to the secondary atomization. The filtered momentum equation (1) is simulated by standard LES approach, with the Smagorinsky closure for the eddy-viscosity. Finally, it is seen from (1) and (5) that two processes in the primary atomization zone are assumed to be fast comparing to resolved turbulent time-scale: it is the variation of liquid flow structure, and the frequency of collisions between detached liquid elements.

Models

Method of floating stochastic particles; computation of $P_l(\vec{x},t)$

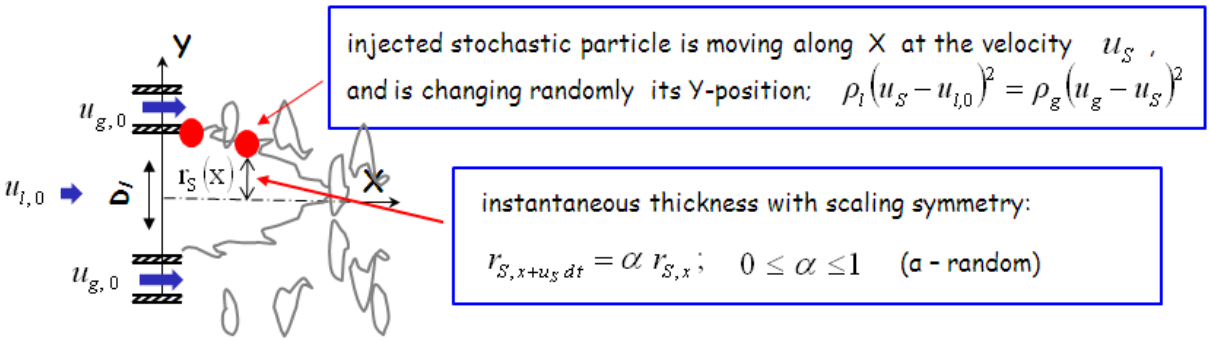

Figure 1: Schematic of floating stochastic particles method

The schematic is presented in Fig 1; the main assumptions are as follows. The floating stochastic particles with zero mass are injected one after another. Each particle proceeds its own path, which ends up after a length of time referred to as the life time of particle: $\tau_l^{-1} = \sqrt{\left|\rho_g u_{g,0}^2 - \rho_l u_{l,0}^2\right| / \rho_l} D_l^{-1}$, where D_l is the initial diameter of the jet. In the down-stream direction x, each stochastic particle moves at constant velocity equal to the convection velocity of interface.

The vertical ordinate of the particle $r_{S,x}$ at different axial positions is assumed to reproduce fractures under scaling symmetry. Then the following stochastic equation is used (Gorokhovski et al.2009):

$$\frac{r_{S,x+u_{l,0}\Delta t}-r_{S,x}}{r_{S,x}}=\left[\langle\ln\alpha\rangle+\frac{\langle\ln^2\alpha\rangle}{2}\right]\frac{\Delta t}{\tau_l}+\sqrt{\frac{\langle\ln^2\alpha\rangle}{2\,\tau_l}}\,dW \tag{6}$$

where $dW(t)$ is the Winner process, $[dW(t)]^2=2\Delta t$, and the choice of $\langle\ln\alpha\rangle$ and $\langle\ln^2\alpha\rangle$ is this: $\langle\ln^2\alpha\rangle/\langle\ln\alpha\rangle=\max(-2;\ln(\lambda_{RT}/\lambda_{KH}))$, $<\ln\alpha>=const\,\ln(\lambda_{RT}/\lambda_{KH})$, where λ_{RT} and λ_{KH} are the most amplified wavelength of the Rayleigh-Taylor and the Kelvin-Helmholtz instabilities, respectively. If the parametric function $\xi(\vec{x},t)$ characterizes the liquid core interface, then the one-point distribution $P_l(\vec{x},t)$ is given by:

$$P_l(\vec{x},t)=\langle\delta(\xi(\vec{x},t)-r_S)d\xi\rangle \tag{7}$$

where the small interval $d\xi$ is associated here with the size of the mesh cell. The spray around the non-depleted liquid core is assumed to be thin. Thereby the computed distribution $P_l(\vec{x},t)$ is attributed to all the liquid around the injector, and the position of blobs to be formed in the near-injector region may be sampled from $P_l(\vec{x},t)$. The illustration of distribution of liquid closely to injector $P_l(\vec{x},t)$ is given on the left-hand side in Fig.2 for $u_{g0}=60\,m/s;\ u_{l0}=0.52\ m/s$. It is seen that although this simulation is based on very simple assumptions, the distribution of liquid closely to injector follows the physical intuition. As to simulation of the interface outwards normal $n_i(\vec{x},t)$ by Brownian motion on the unit sphere (Zamansky et al. 2010), the diffusion coefficient of this motion was taken equal to the life time τ_l. On the right-hand side in Fig. 2, few sample paths of stochastic flowing particle are shown with the simulated outwards normal to interface. It should be noted that $P_l(\vec{x},t)=\langle\delta(\xi(\vec{x},t)-r_S)d\xi\rangle$ and $n_i(\vec{x},t)$ are assumed to be two independent stochastic processes.

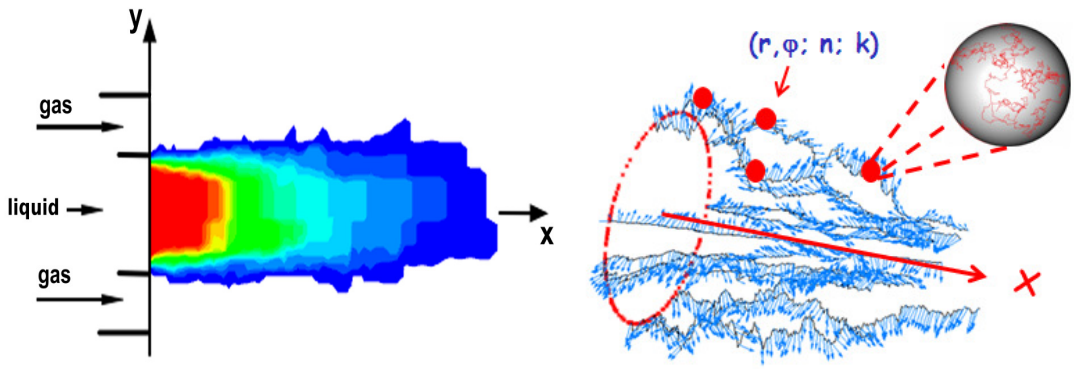

Figure 2: LHS: simulation of the liquid distribution closely to injector with parameters from Hong (2003); RHS: Few sample paths of a stochastic particle: its trajectory defines the instantaneous liquid core boundary; during this path, the instantaneous outward normal is simulated stochastically

Primary liquid blob formation; definition of droplet's statistical temperature

Using simulation of $P_l(\vec{x},t)=\langle\delta(\xi(\vec{x},t)-r_S)d\xi\rangle$, the next step is to sample drop's location in $0<P_l<1$. Along with this position, each formed blob needs to prescribe its size and initial direction. The last one will control the spray opening angle. In this study, the size is sampled from the presumed distribution function:

$f(r) = 1/\lambda_{RT} \exp(-r/\lambda_{RT})$. The sampling procedure of drops is organized in such a way that the injected liquid mass is continuously conserved in drops produced. Similar to Villermaux (1998), but using simulated distribution of $n_i(\vec{x},t)$, the initial angle of drop is given by $\tan\vartheta = n_y u_{l,0}\sqrt{\rho_l/\rho_g}/u_S$. The simplified inter-drop collision model in terms of statistical temperature (per unit mass of drop) T_p/m_p, is described in Chtab & Gorokhovski, 2007. In the present work, T_p/m_p is approximated by kinetic energy of relative liquid-to-gas motion:

$$\frac{T_p}{m_p} = \varepsilon\tau_{St} = \frac{1}{2}\nu_g\left(\frac{\partial\langle u_i\rangle}{\partial x_j} + \frac{\partial\langle u_j\rangle}{\partial x_i}\right)^2 \tau_{St} \tag{8}$$

Another simple closure may be derived from Zaichik & Alipchenkov (2003), Reeks (1977):

$$\frac{T_p}{m_p} = \left(\frac{\nu_{eff}}{\Delta}\right)^2 \frac{1}{1+\tau_{St}\left|S_{ij}\right|} \tag{9}$$

where $\left|S_{ij}\right|$ is the filtered strain rate, and the eddy-viscosity ν_{eff} is given by the Smagorinsky model: $\nu_{eff} = (C_S\,\Delta)^2\,\overline{S}$, $\overline{S} = \left(2\overline{S}_{ij}\overline{S}_{ij}\right)^{1/2}$.

Results and Discussion

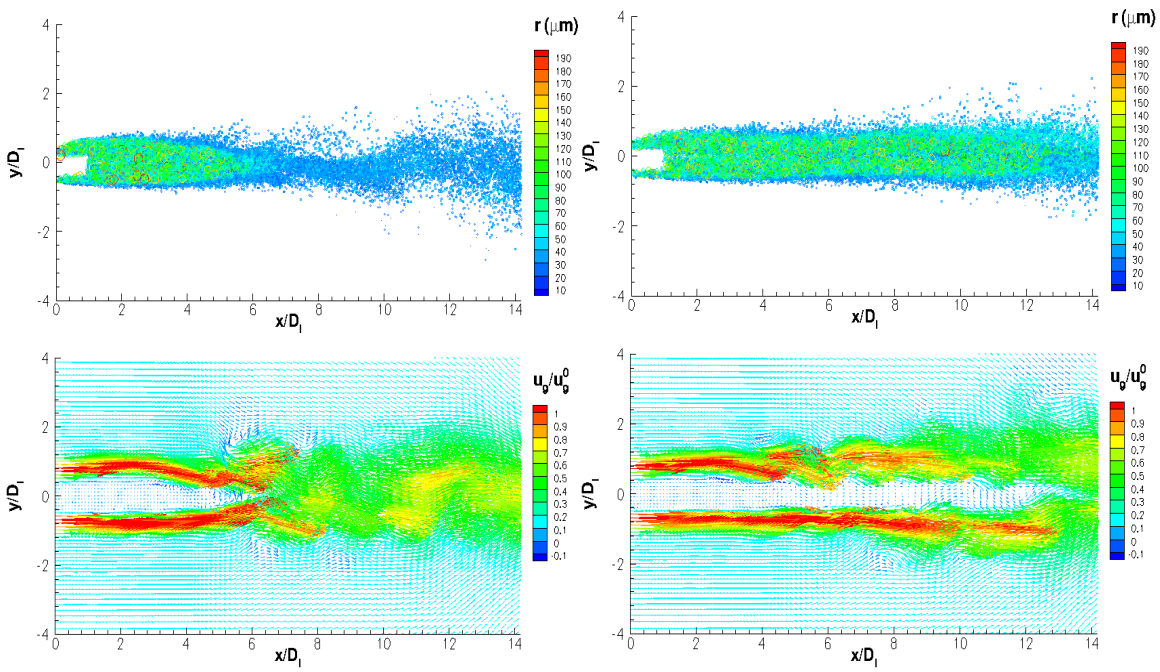

Figure 3: Snapshot of filtered velocity field in the gas flow and the droplet size distribution. Inlet parameters: $u_{g,0} = 60$m/s, $u_{l,0} = 0.52$m/s.

For the same set of input conditions as in Fig.2 corresponding to momentum ratio $M = \rho_g u_{g,0}^2/\rho_l u_{l,0}^2 = 16$, two snapshots of filtered velocity field and spatial distribution of droplet's position-and-size are shown in Fig.3. This figure shows flapping in configuration of liquid core ended up by recirculation

zone in the gas flow. A large spectrum of produced droplets, from 10µm to 200µm, is seen at each spray position. It is also seen that the gas flow is characterized by large scale vortical structures beyond the liquid core. The region close to injector is populated mostly by large drops, with the presence of mist of small stripped droplets. This was also emphasized in experimental observations of Hong (2003). Two similar snapshots, but for higher magnitude of the momentum ratio, $M = 70$ and $M = 220$ (same inlet gas-stream velocity, but smaller inlet velocity of the liquid), are shown in Fig. 4. The increased momentum ratio M leads to the stronger cross-flow exchange of momentum, and consequently, to the more intensive atomization process. Indeed in Fig. 4, one can observe that with increased momentum ratio M, the predicted flow is characterized by the less steepened velocity gradients around the simulated liquid core, and by the finer-grained droplets. The small stripped droplets are then easily to be entrained into the vertical motion in front of the liquid core, in the form of "milky way" filaments. This is seen in Fig. 4. The next pictures assess quantitatively the size and velocity statistics against measurements in Hong, 2003. Fig.5 shows comparison of the mean and the mean Sauter diameter with measurements of Hong (2003) at different gas inlet velocity. When the last one is high the prediction is close to the measurement. The comparison with measurements of the droplet size and velocity along with spray at different distance from its center-line is given in Fig.6 using (8) and (9).

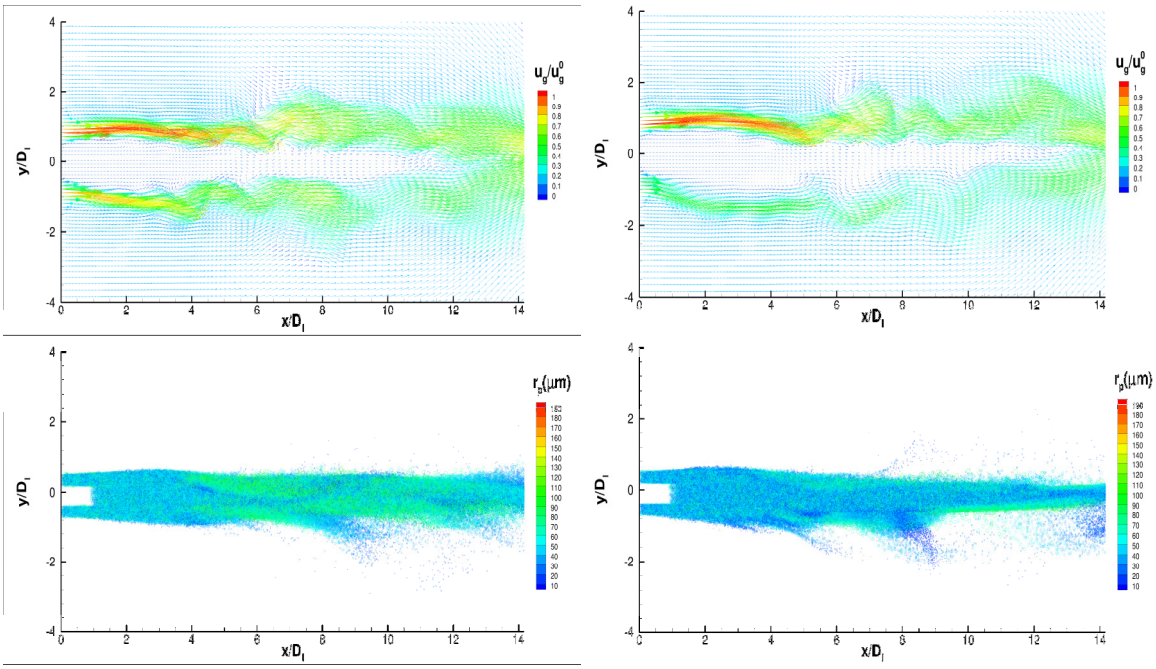

Figure 4: Snapshot of the filtered velocity field in the gas flow, and the droplet's position-and-size distribution; $M = 70$ on the left ; $M = 220$ on the right

References

Apte, S., Gorokhovski, M. &Moin, P. (2003), *Int. J. of Multiphase Flow*, 29, 1503
Beale, J.C. & Reitz, R.D. (1999), *Atomization & Sprays*, 9, 623– 650.
Chtab, A. & Gorokhovski, M. (2007), *Fluids Engineering*, 129, 613–620.
Gorokhovski, M. (2001), Atomization & Sprays, 505–519
Gorokhovski, M.A. & Saveliev, V.L. (2003), Phys. Fluids, 15, 184–192
Gorokhovski, M. & Herrmann, M. (2008), Ann. Rev. Fluid Mechanics, 40, 343–366
Gorokhovski, M., Jouanguy, J. & Chtab, A. (2009), Fluid Dynamics Research, 41
Grigoriadis D.G.E., Bartzis J.G. & Goulas A. (2003), Int. J. Numer. Meth. Fluids, 41 :615-632
Herrmann M. & Gorokhovski M. (2008), CTR, Stanford, Summer Program 2008
Hong, M. (2003), Ph.D. thesis, INPG.
Huh, K. & Gosman, A. (1991), Proceedings of ICMF , Tsukuba, Japan.
Jay, S., Lacas, F. & Candel, S. (2006), Combustion & Flame, 144, 558–577.
Jones W.P. & Lettieri C. (2010), Phys. Fluids, 1070-6631/2010/22
Liu H., Gong X., Li W., Wang F.-C., Yu Z.-H. (2006), Chem. Eng. Sci. 61, 1741
Reeks, M. (1977), JFM, 83, 529.

Tanner, F.X. (2004), Atomisation & Sprays, 14, 211–242.
Vallet, A., Burluka, A. &Borghi, R. (2001), Atomization & Sprays, 11, 619–642.
Villermaux, E. (1998), Propulsion & Power, 14, 807–817.
Yi, Y. & Reitz, R. (2004), Atomization & Sprays, 14, 53–80.
Zaichik, L. & Alipchenkov, V. (2003), Phys. Fluids, 15, 1776.
Zamansky, R., Vinkovkc, I. & Gorokhovski, M. (2010), JoT, 11, 1–18

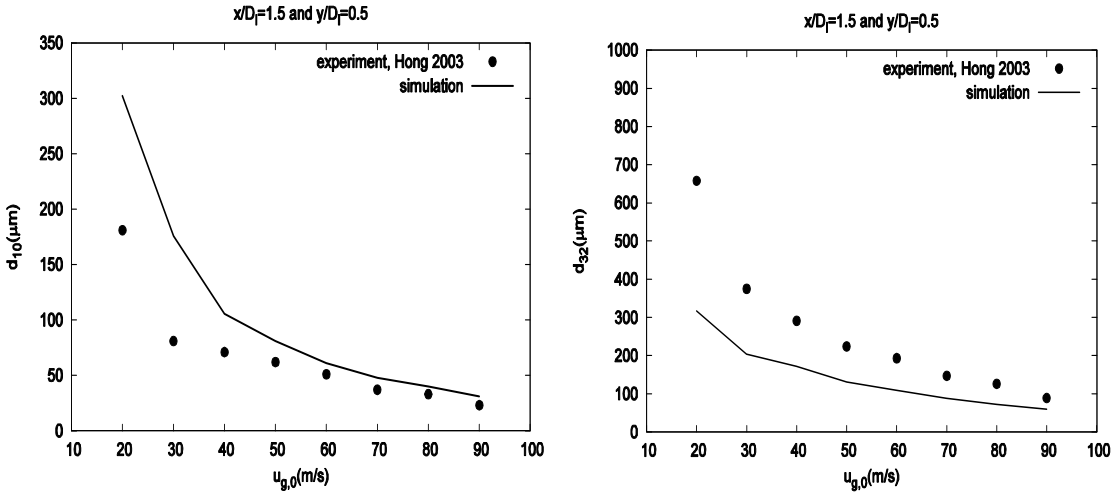

Figure 5: Comparison of the mean diameter d_{10} and the mean Sauter diameter d_{32} at $x/D_l = 1.5$ and $y/D_l = 0.5$, and (M = 16) with measurements (Hong, 2003).

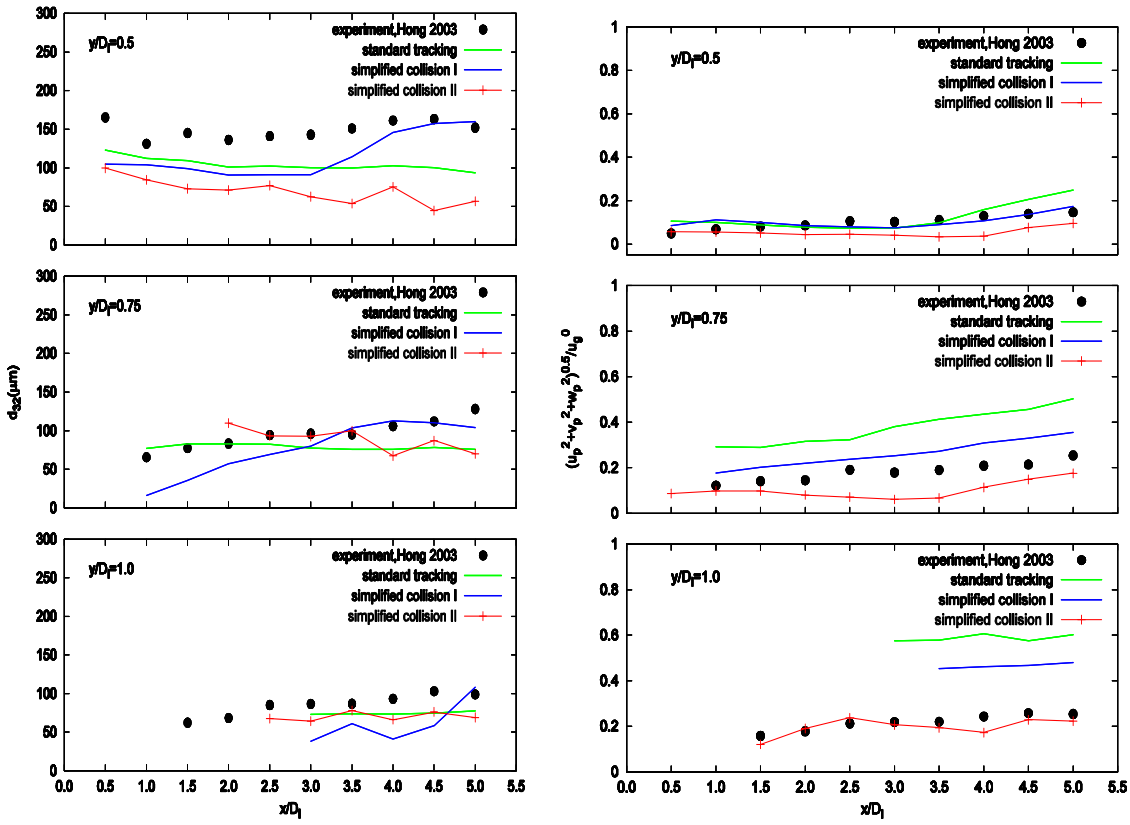

Figure 6: Comparison of the mean Sauter diameter (LHS) and the velocity (RHS) of droplets with measurements (Hong, 2003) at different height along the spray. Inlet parameters: idem as in Fig.3. Simplified collisions I: (8); simplified collisions II: (9); standard tracking: $T_p / m_p = 0$.